RSC Advances

PAPER

View Article Online
View Journal | View Issue

Cite this: *RSC Adv.*, 2015, **5**, 11753

Breaking bonds with electrons: stepwise and concerted reductive cleavage of C–S, C–Se and Se–CN bonds in phenacylthiocyanates and phenacylselenocyanates†

Lydia M. Bouchet,[a] Alicia B. Peñéñory,[a] Marc Robert*[b] and Juan E. Argüello*[a]

Received 10th December 2014
Accepted 22nd December 2014

DOI: 10.1039/c4ra16154h

www.rsc.org/advances

The mechanistic aspects of the electrochemical reduction of phenacylthio- and selenocyanates have been studied. With phenacylthiocyanates (**1**), a change in the reductive cleavage mechanism is observed as a function of the substituent on the phenyl ring. While a stepwise mechanism involving the intermediacy of a radical anion is followed for substrates bearing a strong electron withdrawing group, such as cyano and nitro substituent (**1d**, **1e**), and a concerted mechanism is favoured for compounds bearing an electron-donating or no substituent on the phenyl ring (**1a–c**). A regioselective bond cleavage leads to the fragmentation of the CH_2–S bond with all compounds **1a–e**, further yielding the corresponding 1,4-diketone (**3**) as products. Contrastingly, with phenacylselenocyanates (**2**), two different reductive cleavages occur involving the breaking of both the CH_2–Se and Se–CN bonds. Several products are obtained, all coming from nucleophilic attack at the α (phenacyl) carbon or the selenium atom.

Introduction

The coupling between charge transfer and bond cleavage between two heavy atoms occurs in a large number of chemical, biochemical and catalytic processes, such as cleavage of C–halogen bonds in organic halides, as well as other bonds,[1–4] electron transfer activation of small molecules involved in contemporary energy challenges (such as *e.g.* H_2O, O_2, N_2 and CO_2), as well as enzymatic reactions such as dechlorination processes of RX (X = Cl) toxic derivatives within reductive dehalogenases.[5] In these reactions, the cleavage accompanying charge transfer may be triggered in various manners, electrochemically, by homogenous electron donors or acceptors, photochemically or using pulse radiolysis.[1–3] Charge transfer and bond cleavage reaction may occur concertedly according to a single elementary step (concerted dissociative electron transfer), or in two successive steps, the electron transfer then generating a frangible species that reacts in a distinct, chemical step, as shown in Scheme 1.[1–3]

Potential energy curves describing both reactant and products were modelled by Morse curves, with the assumption that the repulsive interaction of the two fragments formed upon charge transfer is identical to the repulsive part of the reactant Morse curve.[6] Solvent reorganization is calculated from the Marcus–Hush model. These two ingredients of the model lead to a quadratic activation (activation free energy: $\Delta G^{\neq}$) – driving force (minus standard free energy: $-\Delta G^0$) relationship as given in eqn (1):[1–3]

$$\Delta G^{\neq} = \frac{D_{RX} + \lambda_0}{4}\left(1 + \frac{\Delta G^0}{D_{RX} + \lambda_0}\right)^2 \quad (1)$$

where D_{RX} is the homolytic bond dissociation energy and λ_0 the solvent reorganization energy. The standard free energy of the reaction leading to complete dissociation (E: electrode potential, $E^0_{RX/R^{\cdot}+X^-}$: standard potential of the RX/R$^{\cdot}$ + X$^-$ couple) is given by

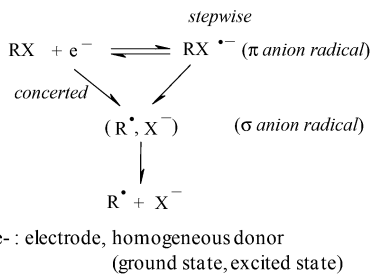

Scheme 1 Dissociative electron transfer mechanisms for the reduction of a substrate RX.

[a]*INFIQC-CONICET-UNC, Dpto. de Química Orgánica, Facultad de Ciencias Químicas, Universidad Nacional de Córdoba, Ciudad Universitaria, X5000HUA Córdoba, Argentina. E-mail: jea@fcq.unc.edu.ar; Web: http://www.fcq.unc.edu.ar/infiqc*

[b]*Université Paris Diderot, Sorbonne Paris Cité, Laboratoired'ElectrochimieMoléculaire, UnitéMixte de RechercheUniversité – CNRS No 7591, Bâtiment Lavoisier, 15 rue Jean de Baïf, 75205 Paris Cedex 13, France. E-mail: robert@univ-paris-diderot.fr*

† Electronic supplementary information (ESI) available. See DOI: 10.1039/c4ra16154h

$$\Delta G^0 = F\left(E - E^0_{RX/R^{\cdot}+X^-}\right) = F\left(E + D_{RX} - T\Delta S^0 - E^0_{X^{\cdot}/X^-}\right) \quad (2)$$

where $E^0_{X^{\cdot}/X^-}$ is the standard potential of the $X^{\cdot}/X^-$ redox couple and ΔS^0 is the bond dissociation entropy and, when required, additional sources of intramolecular reorganization may be included as an additive term to the intrinsic barrier:

$$\Delta G_0^{\neq} = \frac{D_{RX} + \lambda_0}{4} \quad (3)$$

The homolytic bond dissociation energy D_{RX} represents the kinetic penalty for the concerted reaction as compared to the sequential pathway. The electron transfer rates may then be expressed as in the Marcus–Hush theory (eqn (4)):[7–11]

$$k(E) = Z \exp\left[-\frac{D_{RX} + \lambda_0}{4RT}\left(1 + \frac{F\left(E - E^0_{RX/R^{\cdot}+X^-}\right)}{D_{RX} + \lambda_0}\right)^2\right] \quad (4)$$

where Z is the pre-exponential factor.

This set of equations have been successfully applied to both homogeneous and heterogeneous concerted dissociative electron transfers (in the former case, the electrode potential in the driving force expression should be replaced by the standard potential of the molecular electron donor), including C–halogen bonds (alkyl and benzyl halides),[6,12–14] O–O bonds (alkyl peroxides),[15,16] but also N–halogen bonds (*N*-halogenosultams),[17] N–S bonds (sulfonylphthalimides),[18] S–C bonds (sulfonium cations)[19] or S–Cl bonds in arenesulfenyl chlorides.[20,21] It also allowed identifying the competition that exists between the concerted and stepwise pathways, and depends upon intramolecular (structural, electronic) and environmental (solvent, energy of the incoming electron) factors.

Focusing on C–S bonds, the electrochemical reduction of various substituted benzyl thiocyanates showed a change in the cleavage mechanism as a function of the substituent on the benzyl ring.[1,22,23] For the *p*-nitrobenzylthiocyanate, a stepwise dissociative electron transfer mechanism with an anion radical as intermediate takes place, the electron being transitorily located on the π* orbital (largely localized on the nitro groups), before cleavage occurs at the C–S bond. The reduction of the *p*-cyanobenzylthiocyanate follows a concerted charge transfer-bond breaking mechanism, with the electron going directly into the σ* orbital of the C–S bond. With benzyl thiocyanate, the reduction is also concerted with bond cleavage, but cleavage occurs both at the C–S bond (α-cleavage) and at the S–CN bond (β-cleavage).[22,24]

In the case of phenacylthiocyanates, it has been proposed that cathodic reduction at a controlled potential releases $^-$SCN as a leaving group and that after a second electron transfer an enolate ion is formed.[25] This electrogenerated enolate anion acts as a nucleophile to give a 1,4-diketone as the main product. No mechanistic details have been given about the intimate mechanisms for electron transfer and subsequent reactions, notably the degree of association between charge transfer and bond cleavage. On the other hand, the behaviour of phenacylselenocyanates differ from the corresponding sulphur one because the organic selenocyanates undergo a displacement of the CN group by the attack of nucleophilic reagents. It was suggested that the electrogenerated enolate anion formed after the cleavage of the C–Se bond and reduction with a second electron attacks the phenacylselenocyanate to render the (2-phenacylseleno) acetophenone as the main product.[26] Again, no detailed mechanisms were provided.

In this report, we describe the electrochemical reduction of different phenacylthiocyanates (**1**) and phenacylselenocyanates (**2**). The SCN and SeCN groups of **1** and **2** may be considered as pseudohalogen groups. These functional groups can also be used as a masked mercapto/seleno group, as wells as precursors toward the synthesis of sulphur/selenium-containing organic compounds. These later compounds possess a broad range of bioactivities with applications as anticancer agents, and their redox behavior is also interesting because some of them exhibit glutathione peroxidase (GPx) activity.[27–29]

Using both, cyclic voltammetry (CV), theoretical calculations and the model for concerted dissociative electron transfer, we have determined the concerted or stepwise nature of the bond breaking processes and provided a complete analysis of the reduction processes. Various regioselectivity and various mechanisms were encountered. The selected compounds for this study bearing electron donor and withdrawing groups are shown below (Scheme 2).

Results and discussion

Phenacylthiocyanates (**1**) and phenacylselenocyanates (**2**) (Scheme 2) were prepared according to standard procedures. Full characterization of new compounds **1d** and **2d** can be found in the Experimental section and in the ESI† (NMR spectra). The mechanistic analysis was based on the use of the concerted dissociative electron transfer model, in conjunction with insights issued from DFT quantum chemical calculation.

Electrochemical reduction of phenacylthiocyanates (1a–e)

The electrochemical reduction of the phenacylthiocyanates (**1a–e**) was studied by cyclic voltammetry (CV) in *N*,*N*′-dimethylformamide (DMF), in the presence of tetrabutylammonium-tetrafluoroborate (TBAF, 0.1 M) at a glassy carbon electrode. In all cases, the first cathodic wave does correspond to the cleavage of the CH_2–S bond (see below), showing a remarkable regioselectivity for cleavage in the whole family. The peak characteristics

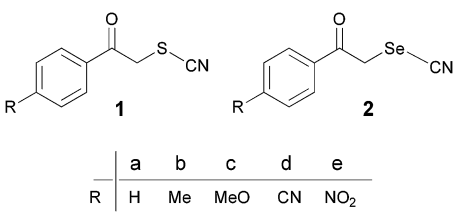

Scheme 2 Phenacylthiocyanates and phenacylselenocyanates investigated.

(peak potential (E_p), peak width ($E_p - E_{p/2}$), slope of E_p *vs.* log(ν) where ν is the scan rate, number of electrons per molecule, and transfer coefficient (α_p)) were obtained for all of these compounds and are given in Table 1.[30,31]

As an example, the CV of phenacylthiocyanate **1a** in DMF displayed an irreversible reduction peak at −1.29 V *vs.* SCE at low scan rate (Fig. 1a). The peak width had a value of 103 mV and the peak potential varied linearly with log(ν) with a slope of 63 mV (Fig. 1b). The transfer coefficient (α_p) values, obtained from peak width (0.46) and from the slope of $\delta E/\delta\log(\nu)$ (0.47), were indicative of a slow electron transfer.[1,2] This first reduction peak corresponds to the consumption of one electron per molecule (by comparison to the monoelectronic wave of ferrocene and taking into account the slow charge transfer).

Scanning in the oxidative direction after the first peak allowed observing an oxidation wave (E_p = 0.79 V *vs.* SCE) similar to the oxidation of $^+NH_4$, ^-SCN (E_p = 0.78 V *vs.* SCE at low scan rate), showing that the thiocyanate anion was formed, and thus the CH_2–S bond was broken during the reduction process. A second reduction peak (reversible) can be seen at lower potentials (−2.03 V *vs.* SCE at low scan rate, Fig. 1a). As shown in Fig. 2, it may correspond to the reduction of acetophenone or alternatively to the reduction of the dimer 1,4-diphenyl-1,4-butanedione (**3a**). It has indeed been reported[25] that the most likely reduction product of **1a** in DMF is the 1,4-diphenyl-1,4-butanedione (**3a**) because the carbon centred radical formed after the CH_2–S fragmentation is immediately reduced at the electrode surface, yielding the corresponding enolate anion, which acts as nucleophile in a subsequent addition process (Scheme 3). This second reduction peak provides a further proof that the CH_2–S bond fragments upon reduction.

Compounds **1b** and **1c** showed similar reduction features with a first, broad, mono electronic reduction peak characterized by slow electron transfer (Fig. S1† and Table 1) and negative reduction potentials (−1.36 to −1.40 V *vs.* SCE at low scan rates). The transfer coefficient values determined from the peak width and from the slope of E_p *vs.* log(ν) plot were 0.46 and 0.37 for **1b**, 0.37 and 0.39 for **1c**, respectively. As with **1a**, the reduction leads to CH_2–S bond fragmentation. The first cathodic peak was followed by a second peak (Table 1), corresponding to the reduction of the 1,4-diketones (1,4-bis(4-tolylbutane-1,4-dione for **1b** and 1,4-bis(4-methoxyphenyl)butane-1,4-dione for **1c**)) obtained after nucleophilic attack of the electrogenerated enolate onto

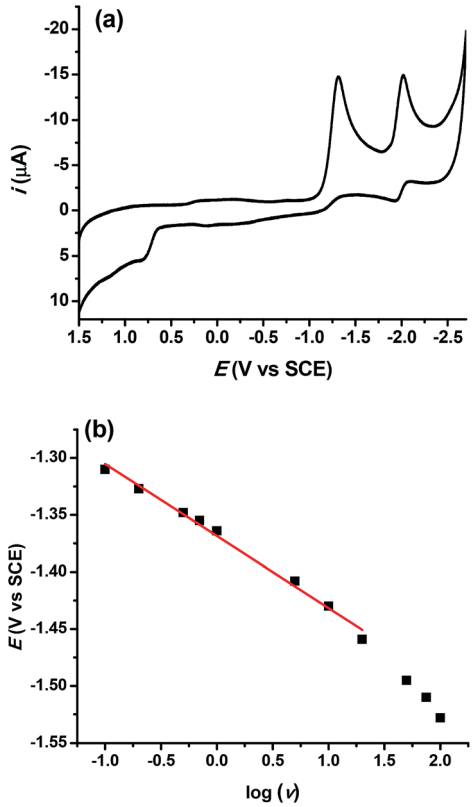

Fig. 1 (a) CV of **1a** (1 mM) in DMF + TBAF (0.1 M) at a glassy carbon electrode, $\nu = 0.1\ Vs^{-1}$. (b) Variation of the peak potential (1st reduction wave) with scan rate.

reactant substrates **1b** and **c** (Scheme 3), similarly to the mechanism followed with **1a**.

Compounds **1d** and **1e** displayed a similar reduction pattern with a first monoelectronic, irreversible reduction peak, but at potentials considerably more positive than those measured with **1a–c** (−0.97 V for **1d** and −0.64 V *vs.* SCE for **1e**, see Table 1 and Fig. S1†). This first reduction wave was also characterized by considerably smaller peak widths (between 60 mV and 80 mV at low scan rates) and smaller peak potential variations with the scan rate (Table 1), indicative of larger transfer coefficient and faster electron transfer. The CH_2–S bond was broken along the reduction wave, as with **1a–c**. However CV's characteristics clearly point toward a different mechanism for cleavage. A second and more negative wave was observed (see Table 1)

Table 1 Electrochemical characteristics of CVs for substituted phenacylthiocyanates (**1**)

$ArCOCH_2SCN$[a]	$E_{p,1}$[b] (V *vs.* SCE)	n[c]	$\delta E_p/\delta\log(\nu)$ slope[d]	α_p[e]	$E_{p/2} - E_p$ (mV)	α_p[f]	$E_{p,2}$[g] (V *vs.* SCE)	E_p $ArCOCH_3$
1a	−1.29	1.2	−63	0.47	103	0.46	−2.03	−2.03
1b	−1.36	0.9	−79	0.37	102	0.46	−2.10	−2.13
1c	−1.39	0.9	−76	0.39	127	0.37	−2.16	−2.19
1d	−0.97	1.2	−59	0.5	80	0.59	−1.47	−1.45
1e	−0.64	1	−39	0.75	60	0.79	−0.85	−0.85

[a] In DMF, TBAF (0.1 M), [**1a–e**] = 1 mM. [b] First reduction peak potential at 0.1 V s^{-1}. [c] Number of electrons exchanged per molecule. [d] mV per unit log(ν). [e] From $E_{p,1}$ *vs.* log(ν). [f] From peak width. [g] Second reduction peak potential.

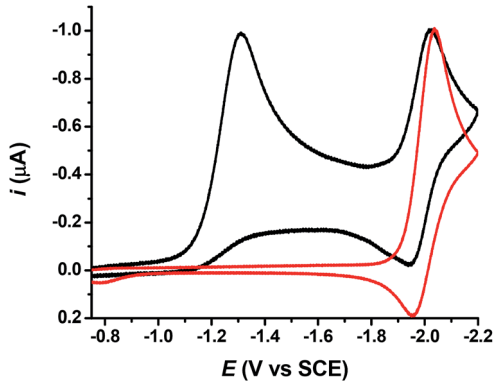

Fig. 2 Cyclic voltammetry of **1a** (1 mM, –) and acetophenone (1 mM, –) in DMF + TBAF (0.1 M) at a glassy carbon electrode, $v = 0.1$ V s^{-1}.

corresponding to the reduction of 1,4-bis(4-cyanophenyl)-butane-1,4-dione (**3d**) and 1,4-bis(4-nitrophenyl)butane-1,4-dione (**3e**), respectively, again similar to compounds **1a–c** (Scheme 3). Further cathodic waves were observed at more negative potentials, due to multielectronic reduction processes of the aromatics (see ESI, Fig. S1†).

Note that in the presence of an excess of phenol, all compounds **1a–e** showed a two electrons stoichiometry at the first reduction peak, in agreement with the proposed reaction mechanism (Scheme 3), in which the enolate was intercepted by the acidic phenol before acting as a nucleophilic agent towards a neutral substrate molecule, thus leading to the use of two electrons per reactant molecule (reactions (1) + (2) in Scheme 3). Note also that these results are in agreement with those previously reported.[25]

Mechanisms for the C–S bond fragmentation

The C–S bond breaking (reaction (1), Scheme 3) may occur in one concerted step or sequentially in two steps through the formation of a transient radical anion, which further undergoes cleavage in a second elementary step. Combining DFT calculations, analysis of CV characteristics and application of the model for concerted dissociative electron transfer allows getting insights in the mechanism as a function of the substituent on the phenyl ring. In the cases of **1a** (Fig. 3), **1b** and **1c**, we were unable to find any minima on the potential energy surface that would correspond to the formation of a radical anion intermediate. Instead, fragmentation occurs at the CH_2–S bond, in agreement with experiments, and a loose adduct between the two fragments, the phenacyl radical and the thiocyanate anion, was identified, as shown for **1a** in Fig. 3 (left). In contrast, with compounds **1d** (Fig. 3, right) and **1e**, a minimum was determined prior to bond breaking, that corresponds to the formation of a radical anion intermediate, with the electronic density mainly localized on the electron withdrawing group borne by the phenyl group (CN for **1d**, NO_2 for **1e**). For compounds **1d** and **1e**, electrochemical data (Table 1) were in agreement with an E + C mechanism, in which a first electron transfer (E) was followed by a fast chemical reaction (C), the breaking of the C–S bond. DFT calculations further confirmed the occurrence of a stepwise mechanism. In other words, reaction (1) (Scheme 3) takes place in two elementary steps. The initial electron was mainly located on the low lying π* orbital of the phenyl ring, owing to the electronic withdrawing substituents (CN, NO_2).

This thermodynamic effect reflects in the peak potentials those were largely positive to the peaks obtained with compounds **1a–c** (the positive shift is roughly 400 mV with **1d** and 700 mV with **1e** as compared to average peak potential

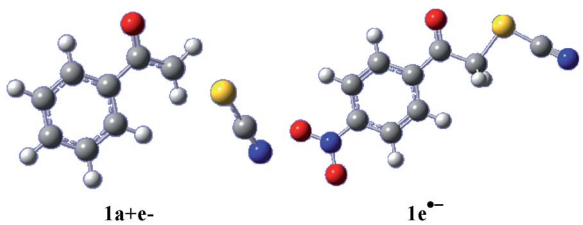

Fig. 3 Left: [phenacyl radical/thiocyanate anion] adduct obtained upon reduction of **1a**. Right: **1e**$^{\bullet-}$ radical anion. Gray: carbon; white: hydrogen; red: oxygen; blue: nitrogen; gold: sulphur.

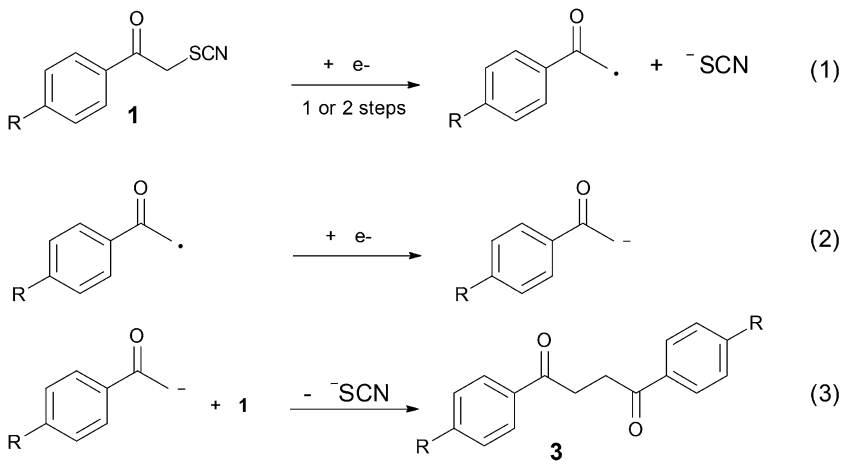

Scheme 3 Electrochemical one electron reduction mechanism for phenacylthiocyanates**1a–e**.

values obtained for **1a–c**). For compounds **1a–c**, DFT calculations suggest a different mechanism, involving a concerted reduction-bond breaking process of the neutral substrate (reaction (1) in Scheme 3 occurs through one single step). The two fragments issued from the cleavage, the phenacyl radical on the one hand and the thiocyanate anion on the other hand were weakly interacting in the gas phase (as illustrated for **1a** in Fig. 3). This weak charge–dipole interaction is likely to be washed out in polar DMF. The CV characteristics were compatible with such a mechanism (Table 1), notably the low values for the electron transfer α, suggesting high values for the reorganization energy. However, more evidence needs to be gathered in order to conclude about the exact mechanism. Using the model for concerted dissociative electron transfer, we may evaluate the transfer coefficient values and compare them to the experimental values. Transfer coefficient is defined through eqn (5):

$$\alpha = \frac{\partial \Delta G^{\neq}}{\partial \Delta G^{0}} = \frac{1}{2}\left(1 + \frac{\Delta G^{0}}{4\Delta G_{0}^{\neq}}\right) \quad (5)$$

where $\Delta G^{\neq}$ is the activation free energy, ΔG^{0} is the standard free energy and $\Delta G_{0}^{\neq}$ is the standard free activation energy obtained at zero driving force. The standard free energy of the reaction leading to complete dissociation is given by eqn (2). In this equation, as well as in eqn (1), E is the electrode potential, D_{RX} is the homolytic bond dissociation energy (C–S bond), ΔS^{0} is the bond dissociation entropy and $E^{0}_{X^{\cdot}/X^{-}}$ is the standard potential of the $X^{\cdot}/X^{-}$ redox couple (X = SCN). This last parameter is equal to 0.75 V *vs.* SCE.[24] λ_0, the solvent reorganization energy, could be estimated through the equivalent radii a of the substrate ($\lambda_0 \approx 3/a$).[1,2] The homolytic bond dissociation energy D_{RX} (C–S bond) and bond dissociation entropy were evaluated by DFT calculations. It also leads to the obtention of the standard free activation energy (intrinsic barrier) through eqn (3). All the data for compounds **1a–c** are given in Table 2.

With these parameters in hand, we were then able to estimate ΔG^{0}, $\Delta G^{\neq}$ at the CV peaks, and then to calculate α. The results obtained at low scan rates are presented in Table 3. A good quantitative match between the experimental (α_{exp}) and calculated (α_{calc}) values was obtained, thus validating a concerted reductive cleavage mechanism of the C–S bond upon first electron reduction. The electron directly goes into the σ* orbital of the carbon–sulphur bond because no low energy hosting orbital was available for generating a radical anion intermediate, in contrast with what is observed for **1d** and **1e**. The very negative reduction potentials (as compared to those measured with **1d** and **1e**) were already clues that the mechanism was likely to be concerted. The single use of DFT calculations cannot lead to the reduction mechanisms, in particular because micro-solvation of the charged species (leaving anion, radical and radical anions) cannot be accurately reproduced, however, they provide a useful tool for confirming that the mechanisms drawn from cyclic voltammetry studies were coherent and plausible.

Table 2 Thermodynamic parameters for the reduction of phenacylthiocyanates **1a–c**

$RC_6H_4COCH_2SCN$	E_p[a]	D_{RX}[b]	ΔS^{0c}; $T\Delta S^{0d}$	a[e]	λ_0[d]
1a R = H	−1.29	46	40.1; 0.52	4.5	0.66
1b R = CH_3	−1.36	45.9	41.0; 0.50	4.7	0.64
1c R = OCH_3	−1.39	45.7	40.4; 0.52	4.7	0.64

[a] V *vs.* SCE at 0.1 V s^{-1}. [b] kcal mol^{-1}. [c] cal mol^{-1}. [d] eV. [e] Å.

Table 3 Thermodynamic and kinetic parameters for the reduction of phenacylthiocyanates **1a–c**

$RC_6H_4COCH_2SCN$	ΔG^{0a}	$\Delta G_0^{\neq a}$	α_{calc}	α_{exp}[b]
1a R = H	−0.564	0.663	0.40	0.47
1b R = CH_3	−0.601	0.657	0.38	0.37
1c R = OCH_3	−0.682	0.655	0.37	0.39

[a] In V, calculated from eqn (2) and (3) at the peak potential (for v = 0.1 V s^{-1}). [b] From Table 1, values obtained from the variation of E_p with log(v).

Electrochemical reduction of phenacylselenocyanates (2)

The electrochemical reduction of the phenacylselenocyanates (**2a–e**) was studied by CV in DMF + TBAF 0.1 M at a glassy carbon electrode. Characteristics for reductive peaks were determined and the results are summarized in Table 4.

The CV of phenacylselenocyanate (**2a**) displayed an irreversible reduction peak at a potential E_p = −1.08 V *vs.* SCE (Fig. 4), with a shoulder close to −0.89 V *vs.* SCE (indicated as $E_{shoulder}$ in Table 4). The irreversible peak observed at −2 V *vs.* SCE corresponds to the reduction of 1,4-bisphenylbutane-1,4-dione (**3a**) (or to the reduction of the substituted acetophenone), as observed in the case of thiocyanate analogue. Cleavage of the CH_2–Se bond was thus likely to occur at the first reduction peak. That selenocyanate anion as the leaving group was confirmed by the observation of an oxidation wave (E_p = 0.59 V *vs.* SCE) similar to that of K^+, $^-$SeCN (E_p = 0.53 V *vs.* SCE). The phenacyl radical $PhCOCH_2^{\cdot}$ obtained after cleavage was reduced at the electrode to the ketone enolate anion ($PhCOCH_2^-$) with a second electron, and this enolate ion reacts with a neutral reactant to provide **3a** (Scheme 4). Another smaller reduction peak was observed at a potential close to −1.48 V *vs.* SCE (Table 4 and Fig. 4). It was ascribed to the reduction of the selenide **4a** (2-(phenacylseleno)acetophenone), which was identified by comparison with an authentic sample (see ESI, Fig. S5†). This result is in agreement with previous studies,[26] in which selenide **4a** may come from nucleophilic attack of the enolate at the selenium atom while releasing cyanide ion as leaving group, as shown in Scheme 4. Alternatively, **4a** may come from a nucleophilic addition of a selenate anion ($PhCOCH_2Se^-$) onto **2a** (Scheme 4). Such a selenate anion could be formed upon cleavage of the Se–CN bond (Scheme 4). The observation of a shoulder just before the main, first reduction peak may be the signature of this reductive cleavage (that does not occur in the thiocyanate family of compounds). Breaking of the Se–CN bond may also lead to the dimer

Table 4 Electrochemical characteristics of CVs for substituted phenacylselenocyanates (2)

$ArCOCH_2SeCN$[a]	$E_{shoulder}$ (V *vs.* ECS)	E_{p1}[b] (V *vs.* SCE)	$\delta E_p/\delta\log(v)$[c]	$E_{p/2} - E_p$ (mV)	E_{p2}[d] (V *vs.* ECS)	E_{p3}[e] (V *vs.* SCE)
2a	−0.89	−1.08	−85	—	−1.48	−2.00
2b	−0.98	−1.09	−155	—	−1.54	−2.10
2c	−1.19	−1.29	−65	—	−1.63	−2.19
2d	—	−0.90	−64	125	−1.27	−1.48
2e	—	−0.57	−54	58	−0.84	−1.47

[a] In DMF + TBAF (0.1 M), [**2a–e**] = 1 mM. [b] First reduction peak potential. [c] mV per unit log(v). [d] Second reduction peak potential. [e] Third reduction peak potential.

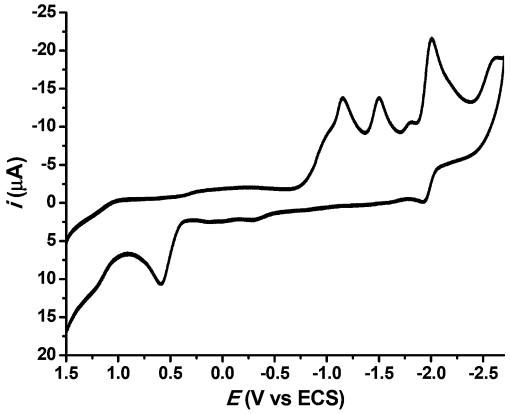

Fig. 4 Cyclic voltammetry of **2a** (1 mM) in DMF + TBAF 0.1 M, $v = 0.1$ V s^{-1}.

compound **5a** (2,2′-diselenediylbis(1-phenylethanone), Scheme 4) by a nucleophilic reaction of the selenate anion at the selenium atom of reactant **2a**. CV of an authentic sample of diselenide **5a** indicated that once formed, it was reduced to **4a** (see ESI, Fig. S5†).

In total, the reduction of **2a** leads to the cleavage of the CH_2–Se bond and to the cleavage of the Se–CN bond, as illustrated in Scheme 4. This non-regioselective reduction process as compared to sulphide analogue **1a** may be ascribed to the fact that the Se–CN cleavage, despite the large Se–CN homolytic bond dissociation energy, may be significantly accelerated by in-cage interactions between the fragments $PhCOCH_2Se^{\bullet}$ and CN^- (charge–dipole interaction). Although studies of these interactions stand beyond the scope of this paper, preliminary quantum calculations indicate that a significant attractive interaction (typically in the order of 0.1 eV) does exist between the selenium centred radical and the cyanide anion, while for the CH_2–Se bond cleavage, there is no interaction between the phenacyl radical and the selenocyanate anion. Note that a sticky interaction in the order of only 1% of D_{C-Se} will result in a decrease of about 15% of the intrinsic barrier for concerted reductive cleavage.[2] Thus, even if the CH_2–Se bond breaking is favoured because of a smaller homolytic bond dissociation energy ($D_{CH_2-Se} = 44$ kcal mol^{-1} $\ll$ $D_{Se-CN} = 90.7$ kcal mol^{-1}, estimated by DFT calculations) both cleavages were observed.

Compounds **2b** and **2c** showed similar peak characteristics (see ESI, Fig. S4†) to compound **2a**. In particular they all presented a first reduction peaks with a shoulder at lower potentials (Table 4). This first peak was followed by a second irreversible peak (−1.54 V *vs.* SCE for **2b** and −1.63 V *vs.* SCE for **2c**), in agreement with the reduction of the corresponding selenides with retention of the Se atom (compounds **4b** and **4c**, Scheme 4). Then, a third irreversible reduction peak corresponding to the reduction of 1,4-bis(4-tolyl)butane-1,4-dione (**3b**) (starting from **2b**) and 1,4-bis(4-methoxyphenyl)butane-

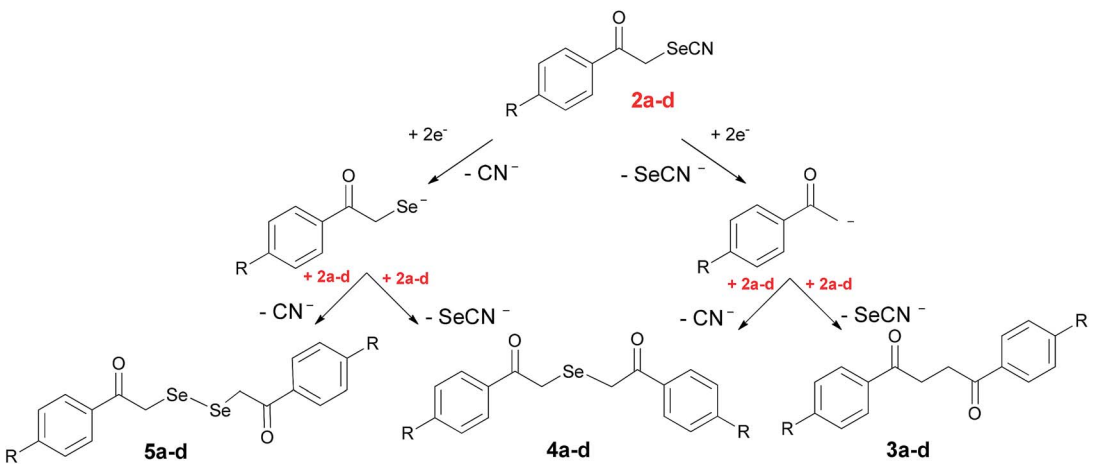

Scheme 4 Mechanism for the electrochemical reduction of phenacylselenocyanates (**2a–d**).

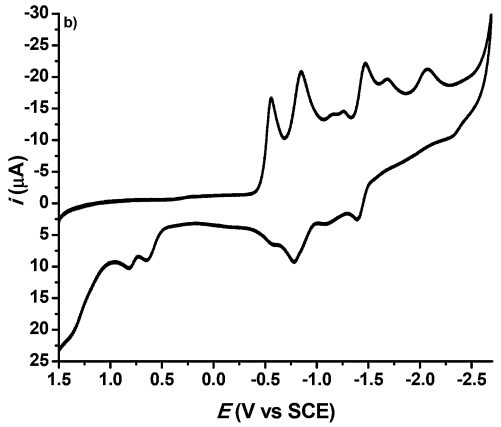

Fig. 5 Cyclic voltammetry of **2e** (1 mM) in DMF + TBAF 0.1 M, $v = 0.1$ V s^{-1}.

1,4-dione (**3c**) (starting from **2c**) could be observed on the CVs. All of these products resulted from nucleophilic attacks as illustrated in Scheme 4. Compound **2d** showed comparable characteristic peaks to **2a–c** compounds (see ESI, Fig. S4†), except that the two reduction processes on the first cathodic wave (C–Se and Se–CN cleavages) almost merge, thus giving a very large peak width (125 mV). As a consequence, the reduction of **2d** led to three products following nucleophilic reactions (Scheme 4).

In this case of *p*-nitrophenacylselenocyanate (**2e**), CVs displayed only a first reduction peak corresponding to consumption of one electron per molecule at a potential of −0.57 V *vs.* SCE (Fig. 5, Table 4), considerably more positive than with compounds **2a–c** (typically 300 to 500 mV more positive). At more cathodic potentials, several reduction waves were observed, which correspond to the reduction of 1,4-bis-(4-nitrophenyl)butane-1,4-dione (**3e**) and for the further reduction of the nitrophenyl ring. Fragmentation of the C–Se bond occurred at the first cathodic peak with no cleavage of the Se–CN bond because the reduction was driven to less negative potential due to the nitro substituent on the phenyl ring, making the Se–CN fragmentation non-competitive.

Conclusions

In conclusion, important mechanistic aspects of the electrochemical reduction of phenacylthio- and selenocyanates have been deciphered. With phenacylthiocyanates (**1**), a striking change in the reductive cleavage mechanism was observed as a function of the substituent on the phenyl ring. In the case of a cyano or a nitro substituent (**1d** and **1e**) a stepwise mechanism involving the intermediacy of the radical anion takes place, while a concerted mechanism is operative with compounds bearing an electron-donating (or no) substituent on the phenyl ring (**1a–c**). CV characteristics, as well as analysis of the voltammograms in terms of transfer coefficient (α) and theoretical calculations both converge towards these conclusions. Remarkably, a regioselective bond cleavage was observed and reductive fragmentation of the CH_2–S bond was followed for all compounds **1a–e**, leading to the corresponding 1,4-diketone (**3**) as products. The latter were formed by an electrochemical-chemical mechanism in which the electrogenerated ketone enolate anions act as nucleophiles in substitution reactions toward **1a–e**, with thiocyanate anion as a leaving group. By contrast, for phenacylselenocyanates **2**, and except in the case of **2e**, which reacts as the sulphur analogue, two different reductive cleavages occur involving breaking of both the C–Se and Se–CN bonds at closely positioned potentials, resulting in the obtention of several products, all coming from nucleophilic attack at the α (phenacyl) carbon or the selenium atom.

Experimental section

General methods

^{1}H, ^{13}C and ^{77}Se NMR spectra were recorded at 400.16, 100.62 and 76.32 MHz respectively on a Bruker 400 spectrometer, and chemical shifts were reported in δ (ppm) relative to TMS with $CDCl_3$ as solvent. HRMS were recorded on a MicroTOF Q II equipment, operated with an ESI source and positive mode, using nitrogen as nebulising and drying gas and sodium formate 10 mM as internal calibrant.

Chemicals

Dimethylformamide (DMF, Aldrich, >99.8%, extra dry over molecular sieves) was used without further purification. Commercially available reagents were used without further purification. Compounds **1a–e** (ref. 32) and **2a–e** (ref. 26) were prepared following literature methods.

p-Cyanophenacylthiocyanate (1d)

White solid.^{1}H NMR (400.16 MHz, $CDCl_3$, 25 °C, TMS): $\delta = 8.05$ (d, $J = 8.8$ Hz, 2H); 7.85 (d, $J = 8.8$ Hz, 2H); 4.69 (s, 2H; CH_2). ^{13}C NMR (100.62 MHz, $CDCl_3$, 25 °C, TMS): $\delta = 189.62$; 136.84; 133; 128.89; 118.10; 117.31; 110.94; 42.3(CH_2). HRMS (ESI^+) calcd for $C_{10}H_7N_2OS$ [M + H] 203.0274, found: 203.0297.

p-Cyanophenacylselenocyanate (2d)

White solid.^{1}H NMR (400.16 MHz, $CDCl_3$, 25 °C, TMS): $\delta = 8.07$ (d, $J = 8.8$ Hz, 2H); 7.85 (d, 2H, $J = 8.4$ Hz); 4.88 (s, 2H, CH_2). ^{13}C NMR (100.62 MHz, $CDCl_3$, 25 °C, TMS): $\delta = 192.1$; 136.6; 133.0; 129.1; 118.1; 117.4; 101.0; 37.3(CH_2). ^{77}Se NMR (76.32 MHz, $CDCl_3$, 25 °C, TMS): $\delta = 168.59$. HRMS (ESI^-) calcd for $C_{10}H_5N_2OSe$ [M − H] 248.9562, found: 248.9560.

Cyclic voltammetry

The electrochemical reduction of the phenacylthiocyanates and phenacylselenocyanates (1 mM) were conducted in a three electrode glass cell, thermostated at 25 °C, under a dry nitrogen or argon atmosphere. The working electrode was a 2 mm diameter glassy carbon electrode (Tokai). It was carefully polished and ultrasonically rinsed with ethanol each time. The reference electrode was a SCE separated from the main solution by a fine porosity glass frit. The counter electrode was a platinum wire. A Methrohm Autolab instrument was used. Positive

feedback correction was applied to minimize the ohmic drop between the working and reference electrode.

Theoretical calculations

Optimizations were carried out using DFT at the B3LYP/6-31+G(d,p) level (and at the B3LYP/6-311+G(d,p) level for the sulphur and selenium atoms).[33] We checked that the conformations obtained were minima by running frequency calculations (no imaginary vibrational frequencies were found). Gas phase optimized energies for compounds **1a-c**, phenacyl radicals and $^{\bullet}$SCN and $^{\bullet}$SeCN were used to estimate homolytic bond dissociation energy values. LUMO calculation, geometries for one electron reduced compounds were calculated in DMF by using the PCM model. All energy values include zero point correction. The calculations were performed using the Gaussian09 package.[34] *Z* matrix and LUMOs for compounds **1a–e**, **2a–e**, radicals and radical anions are given in the ESI.†

Acknowledgements

Authors acknowledge *Ecos-Sud* (grant project A10E03), INFIQC-CONICET and Universidad Nacional de Córdoba (UNC). This work was partly supported by MINCyT-ECOS, CONICET, SECyT-UNC and FONCyT. Compound **5a** was kindly provided by F.R. Bisogno. LMB acknowledges CONICET for the receipt of a fellowship.

Notes and references

1 A. Houmam, *Chem. Rev.*, 2008, **108**, 2190–2237.
2 C. Costentin, M. Robert and J.-M. Savéant, *Chem. Phys.*, 2006, **324**, 40–56.
3 J.-M. Savéant, in *Advances in Physical Organic Chemistry*, ed. T. T. Tidwell, Academic Press, New York, 2000, vol. 35, pp. 117–192.
4 F. W. Maran, D. D. M. Wayner and M. S. Workentin, in *Advances in Physical Organic Chemistry*, ed. T. T. Tidwell, Academic Press, New York, 2001, vol. 36, pp. 85–116.
5 A. Neumann, H. Scholz-Muramatsu and G. Diekert, *Arch. Microbiol.*, 1994, **162**, 295–301.
6 J.-M. Savéant, *J. Am. Chem. Soc.*, 1987, **109**, 6788–6795.
7 N. S. Hush, *Electrochim. Acta*, 1968, **13**, 1005–1023.
8 R. A. Marcus, *Electrochim. Acta*, 1968, **13**, 995–1004.
9 N. S. Hush, *J. Chem. Phys.*, 1958, **28**, 962–972.
10 R. A. Marcus, *J. Chem. Phys.*, 1956, **24**, 966–978.
11 R. A. Marcus, *J. Chem. Phys.*, 1965, **43**, 679–701.
12 K. B. Clark and D. D. M. Wayner, *J. Am. Chem. Soc.*, 1991, **113**, 9363–9365.
13 J.-M. Savéant, *J. Am. Chem. Soc.*, 1992, **114**, 10595–10602.
14 C. P. Andrieux, A. Le Gorande and J. M. Saveant, *J. Am. Chem. Soc.*, 1992, **114**, 6892–6904.
15 M. S. Workentin, F. Maran and D. D. M. Wayner, *J. Am. Chem. Soc.*, 1995, **117**, 2120–2121.
16 S. Antonello, M. Musumeci, D. D. M. Wayner and F. Maran, *J. Am. Chem. Soc.*, 1997, **119**, 9541–9549.
17 C. P. Andrieux, E. Differding, M. Robert and J. M. Saveant, *J. Am. Chem. Soc.*, 1993, **115**, 6592–6599.
18 A. Houmam and E. M. Hamed, *Chem. Commun.*, 2012, **48**, 11328–11330.
19 M. R. Claude, P. Aodrieux, F. D. Saeva and J.-M. Savéant, *J. Am. Chem. Soc.*, 1994, **116**, 7864–7871.
20 C. Ji, M. Ahmida, M. Chahma and A. Houmam, *J. Am. Chem. Soc.*, 2006, **128**, 15423–15431.
21 C. Ji, J. D. Goddard and A. Houmam, *J. Am. Chem. Soc.*, 2004, **126**, 8076–8077.
22 A. Houmam, E. M. Hamed, P. Hapiot, J. M. Motto and A. L. Schwan, *J. Am. Chem. Soc.*, 2003, **125**, 12676–12677.
23 A. Houmam, E. M. Hamed and I. W. Still, *J. Am. Chem. Soc.*, 2003, **125**, 7258–7265.
24 E. M. Hamed, H. Doai, C. K. McLaughlin and A. Houmam, *J. Am. Chem. Soc.*, 2006, **128**, 6595–6604.
25 R. H. B. Batanero, R. Mallmann, M. G. Quintanilla and F. Barba, *Electrochim. Acta*, 2002, **47**, 1761–1764.
26 M. A. D. Otero, B. Batanero and F. Barba, *Tetrahedron*, 2004, **60**, 4609–4612.
27 A. J. Mukherjee, S. S. Zade, H. B. Singh and R. B. Sunoj, *Chem. Rev.*, 2010, **110**, 4357–4416.
28 C. W. Nogueira, G. Zeni and J. B. T. Rocha, *Chem. Rev.*, 2004, **104**, 6255–6286.
29 G. Mugesh and H. B. Singh, *Chem. Soc. Rev.*, 2000, **29**, 347–357.
30 $\alpha = (RT/F)(1.85/E_{p/2} - E_p)$.
31 $\partial E_p/\partial \log(v) = -29.5/\alpha$ at 20 °C.
32 F. R. Bisogno, A. Cuetos, I. Lavandera and V. Gotor, *Green Chem.*, 2009, **11**, 452–454.
33 A. D. Becke, *J. Chem. Phys.*, 1993, **98**, 1372–1377.
34 G. W. T. M. J. Frisch, H. B. Schlegel, G. E. Scuseria, M. A. Robb, J. R. Cheeseman, V. B. G. Scalmani, B. Mennucci, G. A. Petersson, H. Nakatsuji, M. Caricato, X. Li, H. P. Hratchian, A. F. Izmaylov, J. Bloino, G. Zheng, J. L. Sonnenberg, M. Hada, M. Ehara, K. Toyota, R. Fukuda, J. Hasegawa, M. Ishida, T. Nakajima, Y. Honda, O. Kitao, H. Nakai, T. Vreven, J. A. Montgomery Jr, J. E. Peralta, F. Ogliaro, M. Bearpark, J. J. Heyd, E. Brothers, K. N. Kudin, V. N. Staroverov, T. Keith, R. Kobayashi, J. Normand, K. Raghavachari, A. Rendell, J. C. Burant, S. S. Iyengar, J. Tomasi, M. Cossi, N. Rega, J. M. Millam, M. Klene, J. E. Knox, J. B. Cross, V. Bakken, C. Adamo, J. Jaramillo, R. Gomperts, R. E. Stratmann, O. A. J. A. Yazyev, R. Cammi, C. Pomelli, J. W. Ochterski, R. L. Martin, K. Morokuma, V. G. Zakrzewski, G. A. Voth, P. Salvador, J. J. Dannenberg, S. Dapprich, A. D. Daniels, O. Farkas, J. B. Foresman, J. V. Ortiz, J. Cioslowski and D. J. Fox, *Gaussian 09, Revision D.01*, Gaussian, Inc., Wallingford CT, 2013.

